Site-Directed Mutagenesis and Biochemical Analysis of the Endogenous Ligands in the Ferrous Active Site of Clavaminate Synthase. The His-3 Variant of the 2-His-1-Carboxylate Model†

Nusrat Khaleeli, Robert W. Busby,‡ and Craig A. Townsend*

Department of Chemistry, The Johns Hopkins University, Baltimore, Maryland 21218

Received March 8, 2000; Revised Manuscript Received May 11, 2000

ABSTRACT: The facial 2-His-1-carboxylate (Asp/Glu) motif has emerged as the structural paradigm for metal binding in the α-ketoglutarate (α-KG)-dependent nonheme iron oxygenases. Clavaminate synthase (CS2) is an unusual member of this enzyme family that mediates three different, nonsequential reactions during the biosynthesis of the *β*-lactamase inhibitor clavulanic acid. In this study, covalent modification of CS2 by the affinity label *N*-bromoacetyl-L-arginine near His297, which is within the HRV signature of a His-2 motif, suggested this histidine could play a role in metal coordination. However, site-specific mutagenesis of eight His residues to Gln identified His145 and His280, but not His297, as involved in iron binding. Weak homology of His145 and its flanking sequence and the presence of Glu147 fitting the canonical acidic residue of the His−Xaa−Asp/Glu signature are consistent with His145 being a coordinating ligand (His-1). His280 and its flanking sequence, which give poor alignments to most other members of this enzyme family, are similar among a subset of these enzymes and notably to CarC, an apparent oxygenase involved in carbapenem biosynthesis. The separation of His145 and His280 is more than twice that seen in the current 2-His-1-carboxylate model and may define an alternative iron binding motif, which we propose as His-3. These ligand assignments, based on kinetic measurements of both oxidative cyclization/desaturation and hydroxylation assays, establish that no histidine ligand switching occurs during the catalytic cycle. These results are confirmed in a recent X-ray crystal structure of CS1, a highly similar isozyme of CS2 (81% identical). Tyr299, Tyr300 in CS2 modified by *N*-bromoacetyl-L-arginine, is hydrogen bonded to Glu146 (Glu147 in CS2) in this structure and well-positioned for reaction with the affinity label.

In the past decade, the oxygen-activating mononuclear nonheme iron (II) enzymes have emerged as a class of proteins with oxidative capabilities rivaling their heme-dependent counterparts. These versatile enzymes catalyze a diverse array of reactions of physiological, environmental, and pharmaceutical importance (*1*, *2*). A common structural motif for the ferrous active site, the 2-His-1-carboxylate facial triad, is thought to play a crucial role in accommodating different catalytic reactions (*3*). With one face of the octahedral ferrous center occupied by three endogenous protein ligands (His−Xaa−Asp/Glu−Xaa_{53-57}−His), the remaining three cis-oriented sites are available to interact with substrates, α-ketoglutarate (α-KG)[1] and molecular oxygen. This model is a refinement of the earlier His-1 and His-2 motifs identified by Myllyla et al. (*4*).

Nonheme iron oxygenases are central to formation of the *β*-lactam antibiotics penicillin (**2**) and cephalosporin (e.g., **3**) and to the *β*-lactamase inhibitor clavulanic acid (**10**, Scheme 1). Mechanistically, these enzymes carry out reactions in which biosynthetic intermediates are reacted through cyclization and desaturation reactions to highly strained species. The thermodynamic cost of these processes is accounted for in the reduction of molecular oxygen to water (Scheme 1) (*5*). Clavaminate synthase (CS), which is of interest for its pivotal role in the biosynthesis of the potent *β*-lactamase inhibitor clavulanic acid, performs three distinct, nonsuccessive oxidations in the pathway, including a hydroxylation (**5** to **6**) (*6*), an oxidative cyclization (**7** to **8**), and a desaturation reaction (**8** to **9**) (*7*, *8*).

In *Streptomyces clavuligerus*, clavulanic acid (**10**) has been observed to co-occur with penam and cephem metabolites. In fact, the genes encoding their respective biosynthetic proteins including nonheme iron oxygenases isopenicillin N synthase (IPNS) (*9*), deacetoxycephalosporin C synthase (DAOCS) (*10*, *11*), and deacetylcephalosporin C synthase

† This work was supported by a grant from the National Institutes of Health (AI14937).

* To whom correspondence should be addressed at Department of Chemistry, The Johns Hopkins University, 3400 North Charles Street, Baltimore, MD 21218. Phone: 410-516-7444. Fax: 410-261-1233. E-mail: Townsend@jhunix.hcf.jhu.edu.

‡ Present Address: Microbia, 840 Memorial Drive, Cambridge, MA 02139.

[1] Abbreviations: CS, clavaminate synthase; IPNS, isopenicillin N synthase; DAOCS, deacetoxycephalosporin C synthase; DACS, deacetylcephalosporin C synthase; α-KG, α-ketoglutaric acid; DEPC, diethylpyrocarbonate; DTT, 1,4-dithio-D,L-threitol; SDS, sodium dodecyl sulfate; PCR, polymerase chain reaction; TFA, trifluoroacetic acid; CD, circular dichroism; MOPS, 3-(*N*-morpholino)propanesulfonic acid; HPLC, high performance liquid chromatography; PAGE, polyacrylamide gel electrophoresis.

10.1021/bi000534c CCC: $19.00
Published on Web 06/24/2000

Scheme 1

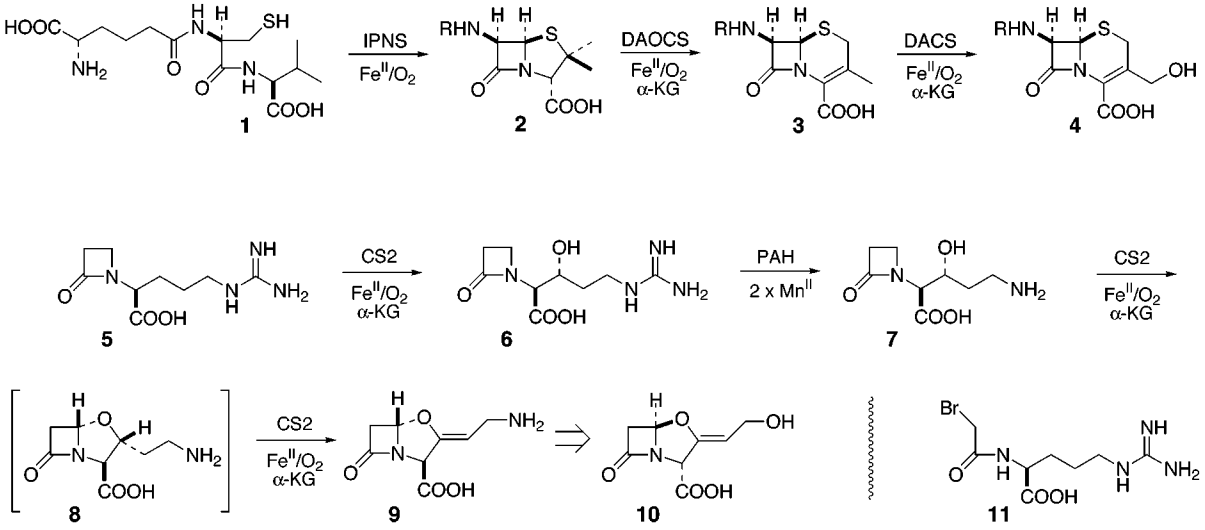

(DACS) (*10*) and clavaminate synthase (CS2) (*12*) map to clusters directly adjacent to each other (*13*). Each of these genes encodes a protein of molecular mass of approximately 35 kDa and uses a single ferrous ion for catalysis (*14*). While the iron-dependent penam/cephem proteins show significant full-length sequence alignments (*15*, *16*), the central enzyme of clavulanic acid biosynthesis, clavaminate synthase (CS), does not align well even within this subclass of nonheme iron (II) enzymes (*12*, *17*).

A high-resolution X-ray crystal structure is available for the α-KG dependent, *β*-lactam antibiotic biosynthetic protein DAOCS (*18*). In the enzyme-metal complex, the ferrous ion is coordinated by His183, His243, and Asp185 and three solvent molecules in a perfect octahedral geometry (*18*) in keeping with the canonical 2-His-1-carboxylate structural motif (*3*). In the ternary DAOCS−Fe(II)−α-KG complex, the cosubstrate binds in a bidentate manner, displacing metal-bound water molecules, an observation similarly borne out during spectroscopic examination of the active site of CS2 (*19*). Biochemical examination of the iron-binding site of CS2 has demonstrated a single monomeric iron center, sensitivity to the histidine-specific reagent diethyl pyrocarbonate (DEPC), and time-dependent inactivation by the affinity label *N*-bromoacetyl-L-arginine (**11**) (*14*). In this paper, we report the loci of covalent modification by this reagent, which took place unexpectedly in the N- and C-terminal regions of CS2. In addition, site-directed mutagenesis of eight histidine residues common between CS2 and its isozyme CS1 [81% identical (*12*)] established two probable ligands to the catalytic iron. These findings reveal an apparent deviation from the presently described 2-His-1-carboxylate model in which the second histidine ligand is located in a new sequence motif that we propose as His-3, and whose separation from His-1 is greater than twice that seen in the current model.

Very recently, an X-ray crystal structure of CS1 has been published with α-KG and either proclavaminate (**6**) or a substrate analogue bound at the active site (*20*). The protein−metal ligands assigned in the course of the presently described mutational experiments are fully in accord with this structure and which afford a partial explanation of the affinity labeling experiments.

EXPERIMENTAL PROCEDURES

Materials. The following were obtained from Sigma Chemical Co. (St. Louis, MO): benzamidine hydrochloride, ammonium sulfate (Grade III), 1,4-dithio-D,L-threitol (DTT), sodium ascorbate, SDS, nalidixic acid, Brij-58, ampicillin, imidazole, Q-Sepharose resin, G-75-50 superfine Sephadex resin. Glass microbeads (0.5 mm) were purchased from VWR (West Chester, PA). Bacto Agar, Yeast Extract, and Bacto Tryptone were purchased from Difco Laboratories (Detroit, MI). Restriction enzymes were obtained from Stratagene (La Jolla, CA) and New England Biolabs (Beverly, MA). *Pfu* DNA polymerase and pBluescript II SK (+) JM101 cells were obtained from Stratagene (La Jolla, CA), and T_4 DNA ligase was obtained from New England Biolabs (Beverly, MA). Acrylamide and *N*,*N*′-methylenebisacrylamide were purchased from Life Technologies, Inc. L-Deoxyguanidino proclavaminic acid (**5**) and *rac*-proclavaminic acid (**7**) were synthesized as described elsewhere (*21*−*24*). The imidazole reagent used for enzyme assays consisted of a 3 M aqueous solution of imidazole (recrystallized 3 times from benzene) adjusted with concentrated HCl to pH 6.8. PCR experiments were performed using a GeneAmp PCR System 2400 (Perkin-Elmer; Norwalk, CT). The pARC306N vector in JM101 cells was a generous gift of Professor C. D. Poulter (University of Utah). Oligonucleotides were synthesized at The Johns Hopkins School of Medicine in the Peptide/Protein Facility, Department of Biological Chemistry.

Affinity Labeling of CS2. Purified CS2 (0.19 mg) was incubated for 2 h at 30 °C with 2 mM [^{14}C]-*N*-bromoacetyl-L-arginine (2.82×10^5 dpm/*μ*mol) in 50 mM MOPS·HCl, pH 7.0, in a total volume of 200 *μ*L. The radiolabeled inactivator was prepared from [1-^{14}C]bromoacetic acid as described earlier (*25*) and purified by HPLC (Whatman Partisil 10-ODS-3, 250 × 9.4 mm; mobile phase: water). The inactivation was stopped by dilution with 4 mL of H_2O. This solution was immediately dialyzed and concentrated to a volume of 50 *μ*L using a Collodion apparatus equipped with a 20 500 molecular weight cutoff membrane.

Lys C Endoproteinase Digestion of Labeled CS2. A digestion mixture containing 50 *μ*L of [^{14}C]-labeled CS2, 50 *μ*L of 0.02% (w/v) endoproteinase Lys C, 350 *μ*L of

Table 1: Sequence of Peptides from Lys C Digestion of CS2 Labeled with *N*-Bromoacetyl-L-arginine

cycle	aa	pmol	cycle	aa	pmol
		$t_r = 13$ min			
1	D	213	12	D	33
2	R	117	13	R	51
3	W	8	14	(N)	5
4	L	95	15	G	12
5	H	39	16	(E)	3
6	R	68	17	(L)	5
7	V	68	18	S	6
8	**X**		19	G	11
9	I	45	20	G	13
10	R	72	21	(E)	4
11	T	39	22	R	14
		$t_r = 22.5$ min			
1	A	927	17	L	283
2	S	486	18	A	161
3	P	456	19	S	30
4	I	497	20	E	51
5	V	468	21	L	126
6	D	314	22	P	39
7	**X**		23	E	71
8	T	185	24	V	33
9	P	152	25	P	65
10	Y	121	26	R	43
11	R	203	27	A	31
12	D	126	28	D	27
13	E	88	29	L	40
14	L	125	30	H	10
15	L	29	31	G	12
16	A	89	32	F	1t

doubly distilled H_2O, and 50 μL of 500 mM ammonium bicarbonate, pH 8.0, was incubated at 37 °C for 24 h and stored at −20 °C until analyzed.

HPLC Determination of Radiolabeled CS2 Peptide Fragments from Proteolysis. An aliquot (150 μL) of the digestion mixture was injected onto a Waters 600 HPLC equipped with a Selectosil C-8 (300 Å) reverse phase HPLC column (250 × 4.6 mm). The mobile phase consisted of a gradient of 100% H_2O to 100% acetonitrile each containing 0.1% TFA at a flow rate of 1 mL/min. Products were monitored at 210 nm. The eluent was collected in 0.5-mL fractions, and radioactivity was determined by scintillation counting. The entire procedure was repeated with the unlabeled affinity label to collect the corresponding peaks for amino acid sequencing.

Amino Acid Sequencing of Peptide Fragments. The purified peptides were derivatized with phenyl isothiocyanate prior to analysis on a Waters PICO-TAG amino acid analysis system. N-terminal sequencing was performed using an Applied Biosystems 470A gas-phase protein sequencer (ABI, Foster City, CA). The following data were obtained for the two peptide fragments of interest having the retention times indicated (Table 1).

Site-Directed Mutagenesis. The *cs2* gene amplified by PCR and cloned into pUC19 *Eco*RI/*Hin*dIII sites served as the plasmid template for mutagenesis, which was carried out with minor modifications to the manufacturer's protocol using the U.S.E. Mutagenesis Kit (Pharmacia Biotech, Inc.; Piscataway, NJ). The eight histidine residues in CS2 that align with those in isozyme CS1 were modified using site-directed mutagenesis by substituting each with glutamine. Some target mutations serendipitously create an easily identifiable change in the restriction pattern of the template and can thus preliminarily be screened for by restriction digest. In the remaining cases, in addition to the target mutation, a second silent mutation was engineered into the oligonucleotide for the same purpose (See Table 2). Sequencing templates were purified with the Plasmid Mini kit (Qiagen; Chatsworth, CA), and all sequencing was accomplished with the PRISM Dye Terminator Cycle-sequencing Ready Reaction kit (ABI, Foster City, CA) and the PE Applied Biosystems 377 Prism DNA Sequencer at the Johns Hopkins School of Medicine Peptide/Protein Facility, Department of Biological Chemistry.

Table 2: Synthetic Oligonucleotides Used for Site-Directed Mutagenesis[a]

aa site	oligonucleotide primers	site change
109	5′-GGTACCCCGT**CTGCAG**ACCGAGC-3′	+ *Pst*I
122	5′-GGTA**CACGTCCTG**GTAGACCGTG-3′	− *Dra*III
131	see text	+ *Bse*RI
145	5′-CATCTCCGTCTG**GAATTC**CAGCAGC-3′	+ *Eco*RI
151	5′-GGAGGATCTGGTACGCCATC-3′	none
167	5′-CCGCCC**GATTC**TCCTGGTCCGCGC-3′	+ *Tfi*I
280	5′-GAACGG**CGTACG**CGCCTGCGTGGT-3′	+ *Bsi*WI
297	5′-GATGTAGACGCG**CTGCAG**CCAG-3′	+ *Pst*I

[a] Sites of mutation are underlined and restriction sites marked in bold. Sites that are both bold and underlined are silent mutations.

Difficult Mutations. The mutation of His131 and 145 was problematic possibly due to secondary structure in this central region of the GC rich *cs2* template (*12*). The His145 mutation was eventually obtained by increased temperatures in the mutagenesis annealing (42 °C) and extension (42 °C) steps in which 25 and 37 °C had been used previously.

To obtain the H131Q mutant, the following manipulations were performed: an *Eco*RI restriction site was created (silent mutation at 429 bp) in *cs2* by site-directed mutagenesis with oligonucleotide 5′-CATCTCCGTGTG**GAATTC**CAGCAG-3′ to yield mutant Eco(+). The 60-bp fragment between the naturally occurring *Dra*III (369 bp) site and the installed *Eco*RI site was excised. Complementary synthetic ca. 60-mers containing the desired target mutation and an additional silent mutation (*Bse*RI) were designed with *Dra*III/*Eco*RI overhangs: 5′-**GTG**TACCCGTCGCCCGGCGCGCAGTAC-CT**CTCCTC**GGAGACCTCCGAGACGCTGCTG**G-**3′ and 5′-**AATTC**CAGCAGCGTCTCGGAGGTCTCC**GAGGA-G**AGGTACTGCGCGCGGGCGACGGGTA**CACGTC**-3′.

After phosphorylation with T_4-polynucleotide kinase (Stratagene) under the manufacturer's conditions, a solution containing 60 pmol of each oligonucleotide was denatured by heating at 100 °C for 5 min. To allow for base pairing between complementary strands, the oligonucleotides were combined and renatured at 65 °C ($T_m = 180$ °C) for 30 min. The oligonucleotide mix, now the insert, was combined with *Dra*III/*Eco*RI linearized Eco(+) DNA in a 10:1 ratio for ligation and subsequent transformation. Plasmid DNA isolated from this pool of transformants was enriched by digestion with *Bse*RI, isolation of linearized (mutant) DNA, religation followed by transformation. Potential mutants were screened for by *Bse*RI digestion and confirmed by DNA sequencing as above.

Construction of the Expression Plasmid. The wild-type and mutant *cs2* genes were subcloned separately into *Nde*I−*Hind*III linearized expression vector pARC306N, which enables high levels of expression of cloned *cs2* in *Escherichia coli* JM101 (*25*).

Expression of the cs2 Genes in E. coli. Cultures of *E. coli* JM101 cells (50 mL) containing the recombinant pARC plasmid were prepared by inoculating single colonies picked from agar plates into liquid medium (LB containing 300 μg of ampicillin/mL) and incubated with shaking at 37 °C overnight. The cultures were diluted into 3 L of TB medium (300 μg/mL ampicillin) in a 1/100 dilution and grown at 37 °C in the Bioreactor MBF (Wheaton) to an optical density at 590 nm (A_{590}) of 1.0. Expression was induced by the addition of nalidixic acid at (50 μg/mL), and expression proceeded at 24 °C for 6 h. The cells were harvested by centrifugation at 4000*g* for 10 min, frozen in liquid N_2, and stored at −80 °C.

Purification of Wild-Type and Mutant CS2 Proteins. Purification of CS2 was performed from 25 g of frozen *E. coli* JM101 cell paste thawed in lysis buffer according to published protocols (*19*) with minor modifications. Buffers were not degassed under nitrogen prior to use. No soy trypsin inhibitor was added to the diluted cell-free extract prior to streptomycin sulfate precipitation. The 70% ammonium sulfate protein pellet was resuspended in 15 mL 50 mM Tris buffer (pH 7.0) containing 1 mM DTT, 1 mM benzamidine, 200 μM PMSF, and 100 μM EDTA and dialyzed against 2000 mL of the same buffer. A linear gradient (1000 mL) of KCl from 0 to 500 mM was used to elute CS2 from the Q-Sepharose column. Following gel filtration, chromatography fractions containing homogeneous CS2, as determined by SDS−PAGE, were pooled and concentrated. Homogeneous CS2 was stored in 50 mM MOPS, pH 7.0, 10% glycerol, and 1 mM DTT and stored at −20 °C.

Activity Assay for CS2, Oxidative Cyclization/Desaturation. Clavaminate synthase activity assays were conducted as described previously (*25*) except that reactions were performed at 23 °C and quenched at 4 min. Relative specific activities were determined with 1 mM *rac*-proclavaminic acid (**7**).

Activity Assay for CS2, Hydroxylation. The standard reaction contained, in a final volume of 250 μL, 0.5 mM DTT, 0.1 mM ascorbate, 1 mM α-KG, 0.05 mM ferrous ammonium sulfate, 0.4 mM L-deoxyguanidino proclavaminic acid (**5**), and 10 μg of CS2 protein. Addition of enzyme was used to initiate reaction, which was incubated at 30 °C for 30 min.

The reaction mixture was filtered through an Ultrafree-MC centrifugal filter unit (Millipore) at 4 °C and analyzed by HPLC on a Phenomenex (Torrance, CA) Prodigy C-18 reverse-phase column (250 × 4.6 mm) eluting with doubly distilled water and monitoring at 210 nm. Deoxyguanidino proclavamic acid (**5**) had a retention time of 13 min, and the hydroxylated product **6** had a retention time of 7.5 min.

Determination of Protein Concentration. Protein concentrations were determined by the method of Bradford (*26*) using bovine serum albumin as the reference standard.

Spectroscopy. CD measurements were made in 0.1-mm cells in a JASCO J-710 spectropolarimeter operated at a scan rate of 20 nm/min in the range 187−260 nm. Protein samples were prepared in 10 mM MOPS (pH 7.0) at a concentration of 1.8 μM.

RESULTS

Affinity Labeling Experiment. The sites of covalent modification of CS2 by *N*-bromoacetyl-L-arginine (**11**) were determined with radiolabeled inactivator. [1-^{14}C]Bromoacetic acid was coupled to L-arginine according to the mixed anhydride method of McKay and Plummer (*14*). CS2 was inactivated by incubation with 2 mM [^{14}C]-*N*-bromoacetyl-L-arginine in MOPS buffer, pH 7.0, for 2 h at 30 °C. Under these conditions, the half-life of CS2 is 50 min. Complete inactivation was not desired to minimize nonspecific alkylation of the enzyme, and so the reaction was quenched after 2 h by a 20-fold dilution with water. The activity of the residual unmodified CS2 was found to be ca. 15%, in keeping with inactivation for slightly more than two half-lives. After concentration and dialysis to remove small molecules by membrane filtration, Lys C protease was used to cleave the labeled enzyme to yield principally 10 peptides upon complete digestion. The proteolysis products were separated by HPLC, and 0.5 mL fractions were collected for scintillation counting. Radioactivity was cleanly concentrated under two peaks outside the solvent front at 13.0 and 22.5 min (Figure 1). On the basis of the specific radioactivity of the [^{14}C]-*N*-bromoacetyl-L-arginine used, the amount of CS2 inactivated, and the counts recovered in the proteolytic fragments, a reaction stoichiometry of 1.0 ± 0.1:1 could be calculated for the fragment retained at 13.0 min and 0.6 ± 0.1:1 for that retained at 22.5 min.

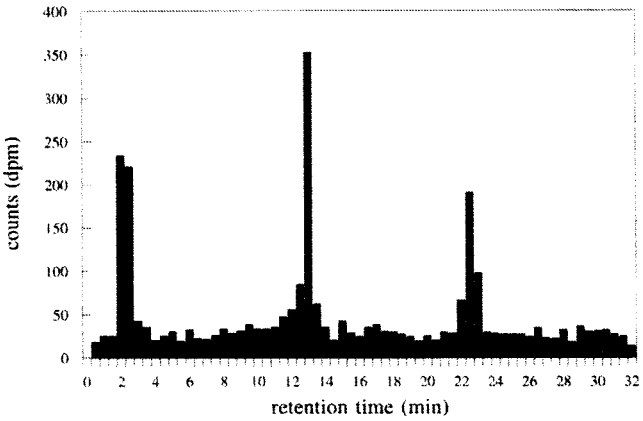

FIGURE 1: Clavaminate Synthase 2 inactivated by [^{14}C]-*N*-bromoacetyl-L-arginine was digested with endoproteinase LysC in a total volume of 500 μL. An aliquot (150 μL) of proteolytic digestion product was resolved by HPLC, and fractions were collected and counted. Figure shows the distribution of counts (dpm) plotted against retention time (min).

The two radiolabeled HPLC peaks were well-separated from other fragments. These were collected in a parallel affinity labeling experiment with unlabeled inactivator and subjected to amino acid sequencing. The sequences of the two peptides corresponding to those giving rise to the radioactive HPLC peaks were CS2 N-terminus (M)ASPIV-D**X**TPYRDELLALASELPEVPRADLHGFLDEAK (38 aa) and CS2 C-terminus DRWLHRV**X**IRTDRNGELSGGER-AGDTISFSPRR (33 aa), where the **X** denotes an unrecognized (modified) residue. Useful sequence was determined for 32 residues of the first peptide above (t_r = 22.5 min; underlined residues) and most of 22 amino acids for the second (t_r = 13.0 min). We assume that only a single amino acid is modified in each peptide fragment. While this assumption is supported by the experimental data, it cannot be strictly concluded for the last few C-terminal residues in each fragment where sequence information became inconclusive.

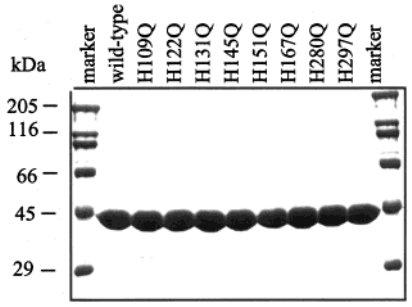

FIGURE 2: SDS−PAGE (12.5% polyacrylamide gel, Coomassie brilliant blue-stained) of purified recombinant CS2 wild type and mutants. Recombinant proteins were prepared as described in Experimental Procedures. Marker, molecular mass standards: 29, 45, 66, 97.4, 116, and 205. From left to right: wild type, His109, His122, His131, His145, His151, His167, His280, and His297 glutamine-substituted mutant CS2 proteins.

We interpret net deviation from the theoretical 1:1 ratio of inactivator/protein to reflect functionally stoichiometric reaction at Tyr300, while less efficient labeling at Cys8 represents a competitive level of nonspecific alkylation at this highly nucleophilic center. Although no histidines were covalently modified, the two residues of CS2 targeted by the affinity label were Cys8 and Tyr300, sites widely separated in the N- and C-terminal regions of the enzyme.

Overexpression of Wild-Type and His-Mutant CS2 Proteins. The covalent modification of residues near the N- and C-termini of CS2 by the affinity label was unexpected considering the high extent of homology in the central portions of the isozymes CS1 and CS2 (*12*). These findings demanded further investigation by site-directed mutagenesis. Eight histidines aligning between isozymes CS1 and CS2 were substituted by glutamine (see Discussion), mutant proteins were obained by standard methods in *E. coli*, and these were purified to homogeneity essentially as previously described (*19*). Pure wild-type and mutant proteins resolved by SDS−PAGE exhibited identical mobilities (Figure 2). As anticipated, the proteins showed very similar physical behavior, especially during ion-exchange chromatography.

Biochemical Analysis of Wild-Type and Mutant CS2 Proteins. The oxidative cyclization/desaturation activities of wild-type CS2 and its mutant enzymes were assayed by derivatization of the reaction product clavaminic acid (**9**) with imidazole following incubation with proclavaminic acid (**7**, Scheme 1) (*14*). A screen of relative activities was performed to investigate which, if any, mutants showed a significant loss of activity. The mutants H109Q, H122Q, H131Q, H151Q, H167Q, and H297Q were found to be catalytically active but less so than the wild-type enzyme. The relative activities of these mutants varied from 10 to 96% of that shown by wild-type CS2 (Table 3). Such a range of catalytic efficiencies has been seen before in similar studies of nonheme iron α-KG dependent oxygenases (*16*, *27*). The results indicated that these six histidine residues do not play essential roles in the catalytic cycle. On the other hand, a complete loss of detectable CS2 activity was found for the mutant enzymes H145Q and H280Q. Comparison of wild-type, the partially active H297Q, and the two inactive mutants by CD spectroscopy revealed no significant conformational difference among the wild-type and mutant proteins (Figure 3).

The oxidative cyclization/desaturation reaction (**7** to **9**, Scheme 1) mediated by CS2 can be conveniently followed by UV assay (*14*). Clavaminate synthase also catalyzes the hydroxylation of **5** to **6**. The latter reaction is significantly more efficient than the former (k_{cat}/K_M 80−85-fold greater) (*28*). In 30-min fixed-time assays, the wild-type and mutants H109Q, H122Q, H131Q, H151Q, H167Q, and H297Q all showed complete conversion of **5** to **6** when monitored by HPLC. In contrast, the two inactive mutants in the oxidative cyclization/desaturation assay, H145Q and H280Q, were observed to give slight, but detectable (<3%) conversion of **5** to its hydroxylated product **6** (data not shown). Together with the CD data noted above, we take this low level of catalysis to imply that the active site structure is largely unchanged from the wild-type in all mutants, and the loss of an endogenous ligand to iron is responsible for the dramatic decrease in catalytic activity seen in the H145Q and H280Q mutants (*29*).

Table 3: Relative Activities of CS2 His → Gln Mutants[a]

protein	rel act. (%)
wild-type	100
His 109	83
His 122	96
His 131	16
His 145	0
His 151	10
His 167	95
His 280	0
His 297	65

[a] Error ± 1%.

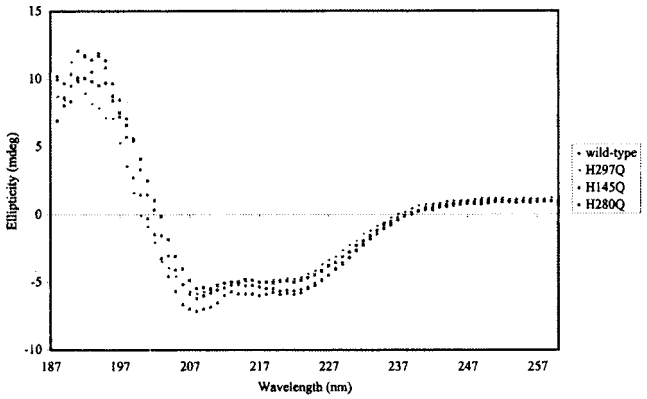

FIGURE 3: CD spectra of CS2 wild type, H297Q, H145Q, and H280Q mutant proteins. Each protein sample of concentration 1.8 μM in 10 mM MOPS, pH 7.0, was scanned five times from 260 to 187 nm.

DISCUSSION

The trifunctional oxygenase clavaminate synthase provides a striking example of the diverse oxidative capability manifested by the α-KG dependent, nonheme iron (II) enzymes (Scheme 1). The catalytic versatility of the enzymes in this class has been attributed to fine-tuning of ferrous active site reactivity as determined by the choices of endogenous (protein) and exogenous (substrate, cofactor, and dioxygen) ligands and by the binding flexibility provided by three cis-oriented sites available on one face of the octahedral coordination sphere of iron (*1*). For these reasons, there has been a longstanding interest in identifying the critical residues involved in iron binding in this enzyme in comparison to other members of the nonheme iron

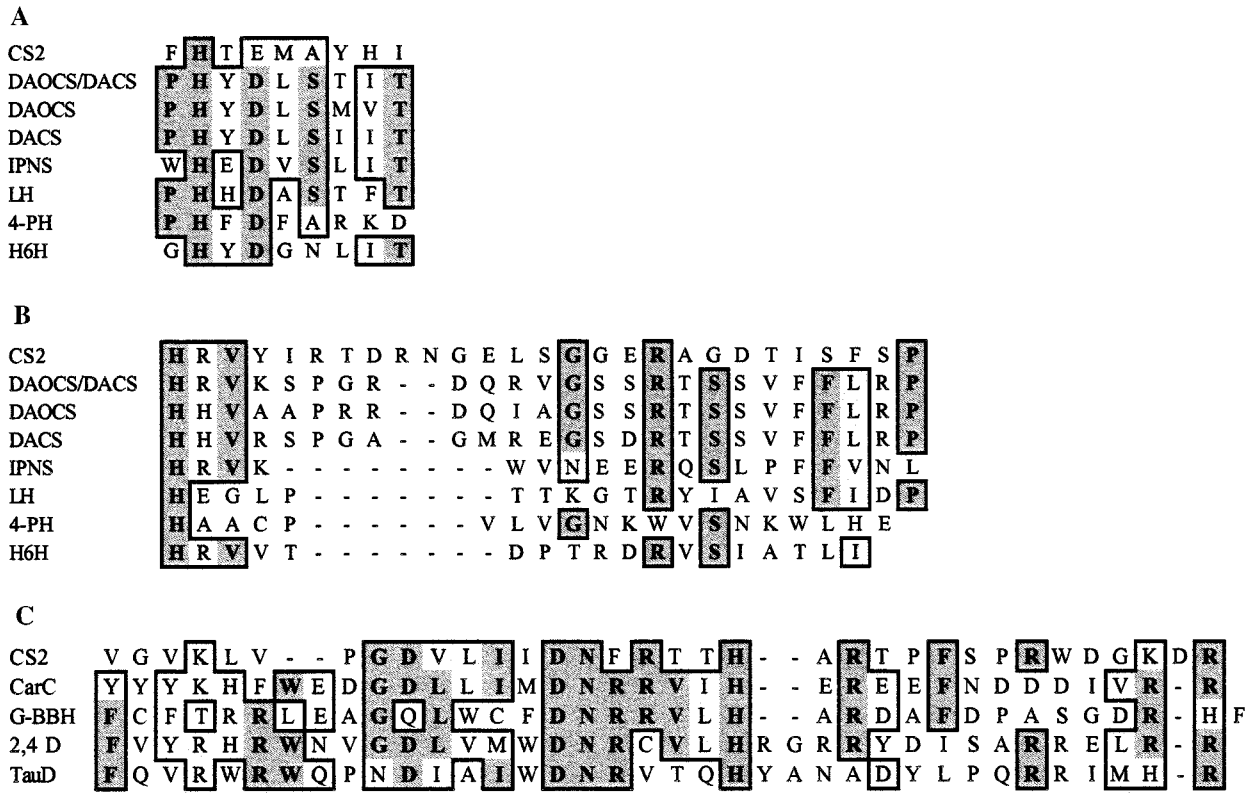

FIGURE 4: In CS2, the putative His-1 motif begins with residue 144, and the His-2 motif begins with residue 297. Results are shown for CS2 from *Streptomyces clavuligerus* (*12*), DAOCS/DACS from *Cephalosporium acremonium* (*38*), DAOCS from *Streptomyces clavuligerus* (*11*), DACS from *S. clavuligerus* (*10*), IPNS from *Penicillium chrysogenum* (*39*), lysyl hydroxylase (LH) from chick (*40*), prolyl-4-hydroxylase (4-PH) α-subunit from human (*41*), and hyoscyamine 6β-hydroxylase (H6H) from *Hyoscyamus niger* (*42*). In CS2, the His-3 motif begins with residue 261. Results are shown for CS2 from *S. clavuligerus* (*12*), CarC from *Erwinia carotovora* (*33*), γ-butyrobetaine hydroxylase from *Pseudomonas* sp. AK1 (*43*), 2,4-dichlorophenoxyacetate monooxygenase from *Alcaligenes eutrophus* (*34*), and taurine dioxygenase from *E. coli* (*35*). (A) His-1 motif; (B) His-2 motif; and (C) His-3 motif. Invariant residues are shaded and boxed, and similar residues are lightly shaded and boxed.

oxygenases. These residues in CS2 could not be located by full-length sequence alignments.

Much information about CS2 has accrued from kinetic studies (*23*), spectroscopic analyses (*19*), and chemical modification by standard reagents such as diethylpyrocarbonate and *N*-ethylmaleimide (*14*). We utilized the affinity label *N*-bromoacetyl-L-arginine (**11**), which causes irreversible, time-dependent, and parallel loss of each CS2-catalyzed reaction (*14*). Among the 10 fragments obtained by LysC digestion of affinity-labeled CS2, only the N- and C-terminal proteolysis products were targeted. The significance of the N-terminal Cys8 modification is not fully known, but is thought to reflect nonspecific alkylation of CS2. In contrast, Tyr300, the second CS2 site targeted by the affinity label, reacts stoichiometrically and is adjacent to His297. This histidine is within the HRV signature of the recognized His-2 motif. Although this residue is distal to the highly conserved central regions of the isozymes CS1 and CS2, the results suggested that His297 might be a ligand for iron binding.

To directly establish the identity of the endogenous ligands to iron in CS2, site-directed mutagenesis experiments were undertaken. In these experiments, the choice of glutamine to replace histidine was deliberate. Statistical analysis of naturally occuring mutations in protein families where function is conserved has indicated that glutamine is one of the most frequent substitutions for histidine (*30*). Moreover, in keeping with these empirical findings, calculations indicate the hydropathy indices of histidine and glutamine are quite similar (*31*). Replacement of histidines with glutamine is considered among the least likely choice to cause activity losses due to significant conformational changes in the mutant proteins, thus minimizing unnecessary complications in functional analysis. Physical characterization of the wild-type and mutant proteins by CD spectroscopy confirmed that no gross conformational changes occurred in any of the proteins studied (data not shown and Figure 3).

Primary sequence alignment of α-KG-dependent, nonheme iron-requiring enzymes has revealed two conserved histidine-containing signature sequences. These were termed the His-1 and His-2 motifs (*4*). This analysis has been further refined from the examination of two X-ray crystal structures (*18*, *32*) and the primary sequences of more than 40 nonheme iron α-KG dependent oxygenases to place their separation in the 2-His-1-carboxylate model at 55−59 residues (*3*). Although H297 falls in the HRV signature sequence identified for the His-2 motif and lies very close to Tyr300 modified by *N*-bromoacetyl-L-arginine (**11**) (Figure 4B), mutation of this residue did not result in significant loss of catalytic activity, and it is not a ligand to iron (Table 3).

In keeping with its location in a weakly homologous His-1 motif (Figure 4A), mutation of His145 resulted in the loss of detectable CS2 activity. Mutation of a second histidine, His280, gave similar loss of CS2 activity (Table 3). Attempted alignment of the latter residue with a collection of other nonheme iron α-KG dependent oxygenases failed to show any convincing homology at this site. However, closer

examination of this immediate region in comparison to other available primary sequence data revealed an unexpected correlation to CarC, a gene product thought to be involved in an oxidative step in the biosynthesis of the carbapenem β-lactam antibiotics (Figure 4C) (*33*). Surprisingly, a subset of α-KG-dependent, nonheme iron oxygenases including (2,4-dichlorophenoxy)acetate dioxygenase (*34*) and taurine dioxygenase (*35*), which have been thought to obey the current 2-His-1-carboxylate model based only on sequence data (*36*, *37*), was also found in the present alignment. While site-specific mutagenesis experiments have not identified the true metal ligands in any of the proteins aligning to CS2 in Figure 4C, we propose that this finding may represent a new motif of iron binding in a variation on the 2-His-1-carboxylate structural theme.

We entertained the possibility that perhaps to accommodate three substrates and three dissimilar oxidative reactions, the protein may exist in equilibrium between two iron-bound states, for example, His145 and His280 for oxidative cyclization/desaturation and His145 and His297 for hydroxylation given the much greater local homology observed in the vicinity of His297. However, when hydroxylation by the CS2 mutants was monitored, H297Q was quite active and only a trace of reaction could be detected for H145Q and H280Q, in complete accord with the results of the cyclization/desaturation assay. As has been previously noted in a related context (*29*), the very low hydroxylation activity of the mutated histidine residues assigned to iron coordination may be taken to reflect loss of an endogenous ligand rather than unfavorable protein conformational effects.

Therefore, CS2 mediates three nonsequential oxidative reactions at a single ferrous active site where two histidine ligands, His145 and His280, remain unchanged throughout the catalytic cycle. We tentatively assign the third endogenous Fe(II) ligand to Glu147 in accord with the 2-His-1-carboxylate model (*3*). In this model, the separation of the histidine ligands to iron falls in a narrow range of 55−59 residues in more than 40 nonheme iron oxygenases. The distance between the two actual histidine metal ligands in CS2 is 134 amino acids, more than twice this value. While His145 obeys the canonical His-1 site motif, His280 does not resemble the expected His-2 motif. The latter sequence context is clearly detectable for His297, but site-specific mutation at this locus does not support its being a ligand to iron. In contrast, His280, although not showing convincing homology to most members of the α-KG dependent, nonheme oxygenases, reveals similarity to a small subset of these enzymes, most notably CarC whose proposed function in carbapenem biosynthesis is oxidative. Interestingly, the separation of the two histidines aligning with His145 and His280 in CarC is 140 residues, quite similar to that in CS2. For all the examples in Figure 4C, the separation of the histidine ligands in full-length protein alignments is 145 ± 10 amino acids. We propose this subset of nonheme iron oxygenases may define a His-3 motif. For the case of CS2, this structural change may be required to modulate the reactivity of the active site to accommodate substrates bearing amino and guanidino side chains as well as carrying out hydroxylation, oxidative cyclization, and desaturation chemistry. Further experiments will be required to determine the generality of this variant of the 2-His-1-carboxylate model.

The X-ray crystal structure of CS1 has recently been published with α-KG and either proclavminate (**6**) or *N*-acetyl-L-arginine bound at the active site (*20*). This structure confirms the identities of His145 and His280 as the histidine ligands to iron and the predicted coordination of Glu147 in CS2 (His144, His 279, and Glu146 in CS1). As pointed out by these authors, the choice of glutamate, as opposed to the nearly universally observed aspartate at this locus, may afford needed flexibility at the iron site to accommodate the three oxidative reactions mediated by CS. Moreover, Tyr299 (Tyr300 in CS2), the principal site of covalent modification by the affinity label *N*-bromoacetyl-L-arginine is hydrogen bonded in the X-ray crystal structure of CS1 to Glu146 (Glu147 in CS2) and is well-positioned to carry out nucleophilic substitution of this acyl halide. The static view of CS1 provided by the X-ray crystallographic analysis is thus found to be fully in keeping with the dynamic solution behavior of CS2 in all three of its catalytic reactions.

ACKNOWLEDGMENT

We thank B. O. Bachmann and W. L. Kelly for the synthesis of substrates used in the enzyme assays. We are grateful to the laboratory of Professor E. Friere in the Department of Biology at The Johns Hopkins University for use of the spectropolarimeter and to Dr. J. H. Stillman for help obtaining the CD data.

REFERENCES

1. Que, L., Jr., and Ho, R. Y. N. (1996) *Chem. Rev. 96*, 2607−2624.
2. Feig, A. L., and Lippard, S. J. (1994) *Chem. Rev. 94*, 759−805.
3. Hegg, E. L., and Que, L., Jr. (1997) *Eur. J. Biochem. 250*, 625−629.
4. Myllyla, R., Gunzler, V., Kivirikko, K. I., and Kaska, D. D. (1992) *Biochem. J. 286*, 923−927.
5. Townsend, C. A. (1993) *Biochem. Soc. Trans. 21*, 208−213.
6. Baldwin, J. E., Lloyd, M. D., Wha-Son, B., Schofield, C. J., Elson, S. W., Baggeley, K. H., and Nicholson, N. H. (1993) *J. Chem. Soc., Chem. Commun.*, 500−502.
7. Elson, S. W., Baggeley, K. H., Gillett, J., Holland, S., Nicholson, N. H., Sime, J. T., and Woroniecki, S. R. (1987) *J. Chem. Soc., Chem. Commun.*, 1736−1740.
8. Salowe, S. P., Marsh, E. N., and Townsend, C. A. (1990) *Biochemistry 29*, 6499−6508.
9. Leskiw, B. K., Aharonowitz, Y., Mevarech, M., Wolfe, S., and Vining, L. C. (1988) *Gene 62*, 187−196.
10. Kovacevic, S., and Miller, J. R. (1991) *J. Bacteriol. 173*, 398−400.
11. Kovacevic, S., Weigel, B. J., Tobin, M. B., Ignolia, T. D., and Miller, J. R. (1989) *J. Bacteriol. 171*, 754−760.
12. Marsh, E. N., Chang, M. D.-T., and Townsend, C. A. (1992) *Biochemistry 31*, 12648−12657.
13. Ward, J. W., and Hodgson, J. E. (1993) *FEMS Microbiol. Lett. 110*, 239−242.
14. Busby, R. W., and Townsend, C. A. (1996) *Bioorg. Med. Chem. Lett. 4*, 1059−1064.
15. Roach, P. L., Clifton, I. J., Fulop, V., Harlos, K., Barton, G. J., Hadju, J., Andersson, I., Schofield, C. J., and Baldwin, J. E. (1995) *Nature 375*, 700−704.
16. Borovok, I., Landman, O., Kreisberg-Zakarin, R., Aharonowitz, Y., and Cohen, G. (1996) *Biochemistry 35*, 1981−1987.
17. Lloyd, M. D., Merritt, K. D., Lee, V., Sewell, T. J., Wha-son, B., Baldwin, J. E., and Schofield, C. J. (1999) *Tetrahedron 55*, 10201−10220.
18. Valegard, K., Terwisscha von Scheltinga, A. C., Lloyd, M. D., Hara, T., Ramaswami, S., Perrakis, A., Thompson, A., Lee,

H.-J., Baldwin, J. E., Schofield, C. J., Hadju, J., and Andersson, I. (1998) *Nature 394*, 805−809.
19. Pavel, E. G., Zhou, J., Busby, R. W., Gunsior, M., Townsend, C. A., and Solomon, E. I. (1998) *J. Am. Chem. Soc. 120*, 743−753.
20. Zhang, Z., Ren, J., Stammers, D. K., Baldwin, J. E., Harlos, K., and Schofield, C. J. (2000) *Nat. Struct. Biol. 7*, 127−133.
21. Wu, T. K., Busby, R. W., Houston, T. A., McIlwaine, D. B., Egan, L. A., and Townsend, C. A. (1995) *J. Bacteriol. 177*, 3714−3720.
22. Townsend, C. A. (1993) *Biochem. Soc. Trans. 21*, 208−213.
23. Salowe, S. P., Krol, W. J., Iwata-Reuyl, D., and Townsend, C. A. (1991) *Biochemistry 30*, 2281−2292.
24. Krol, W. J., Mao, S.-s., Steele, D. L., and Townsend, C. A. (1991) *J. Org. Chem. 56*, 728−731.
25. Busby, R. W., Chang, M. D.-T., Busby, R. C., Wimp, J., and Townsend, C. A. (1995) *J. Biol. Chem. 270*, 4262−4269.
26. Bradford, M. M. (1976) *Anal. Biochem. 72*, 248−254.
27. Tan, D. S. H., and Sim, T.-S. (1996) *J. Biol. Chem. 271*, 889−894.
28. Baldwin, J. E., Lloyd, M. D., Wha-Son, B., Schofield, C. J., Elson, S. W., Baggaley, K. H., and Nicholson, N. H. (1993) *J. Chem. Soc., Chem. Commun.*, 500−502.
29. McGinnis, K., Ku, G. M., VanDusen, W. J., Garsky, V., Fu, J., Garsky, V., Stern, A. M., and Friedman, P. A. (1996) *Biochemistry 35*, 3957−3962.
30. Dayhoff, M. O., Eck, R. V., and Park, C. M. (1972) in *Atlas of Protein Sequence and Structure* (Dayhoff, M. O., Ed.) pp 89−99, National Biomedical Research Foundation, Washington, DC.
31. Kyte, J., and Doolittle, R. F. (1982) *J. Mol. Biol. 157*, 105−132.
32. Serre, L., Sailland, A., Sy, D., Boudec, P., Rolland, A., Pebay-Peyroula, E., and Cohen-Addad, C. (1999) *Structure 7*, 977−988.
33. McGowan, S. J., Sebaihia, M., Porter, L. E., Stewart, G. S. A. B., Williams, P., Bycroft, B. W., and Salmond, G. P. C. (1996) *Mol. Microbiol. 22*, 415−426.
34. Streber, W. R., Timmis, K. N., and Zenk, M. H. (1987) *J. Bacteriol. 169*, 2950−2955.
35. van der Ploeg, J. R., Weiss, M. A., Saller, E., Nashimoto, H., Saito, N., and Kertesz, M. A. (1996) *J. Bacteriol. 178*, 5438−5446.
36. Ryle, M. J., Padmakumar, R., and Hausinger, R. P. (1999) *Biochemistry 38*, 15278−15286.
37. Hegg, E. L., Whiting, A. K., Saari, R. E., McCracken, J., Hausinger, R. P., and Que, L., Jr. (1999) *Biochemistry 38*, 16714−16726.
38. Samson, S. M., Dotzlaf, J. E., Slisz, M. L., Becker, G. W., Van Frank, R. M., Veal, L. E., Yeh, W.-K., Miller, J. R., Queener, S. W., and Ingolia, T. D. (1987) *Biotechnology 5*, 1207−1211.
39. Carr, L. G., Skatrud, P. L., Scheetz, M. E., II, Queener, S. W., and Ingolia, T. D. (1986) *Gene 48*, 257−266.
40. Myllyla, R., Pihlajaniemi, T., Pajunen, L., Turpeenniemi-Hujanen, T., and Kivirikko, K. I. (1991) *J. Biol. Chem. 266*, 2805−2810.
41. Helaakoski, T., Vuori, K., Myllyla, R., Kivirikko, K. I., and Pihlajaniemi, T. (1989) *Proc. Natl. Acad. Sci. U.S.A. 86*, 4392−4396.
42. Matsuda, J., Okabe, S., Hashimoto, T., and Yamada, Y. (1991) *J. Biol. Chem. 266*, 9460−9464.
43. Ruetschi, U., Nordin, I., Odelhog, B., Jornvall, H., and Lindstedt, L. (1993) *Eur. J. Biochem. 213*, 1075−1080.

BI000534C